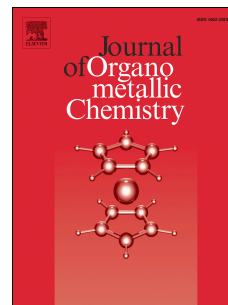


# Accepted Manuscript

Synthesis, structural characterization, DNA binding and antioxidant potency of new ferrocene incorporated acyl ureas

Faiza Asghar, Amin Badshah, Raja Azadar Hussain, Manzar Sohail, Kamran Akbar, Ian Sydney Butler



PII: S0022-328X(15)30113-3

DOI: [10.1016/j.jorganchem.2015.08.010](https://doi.org/10.1016/j.jorganchem.2015.08.010)

Reference: JOM 19198

To appear in: *Journal of Organometallic Chemistry*

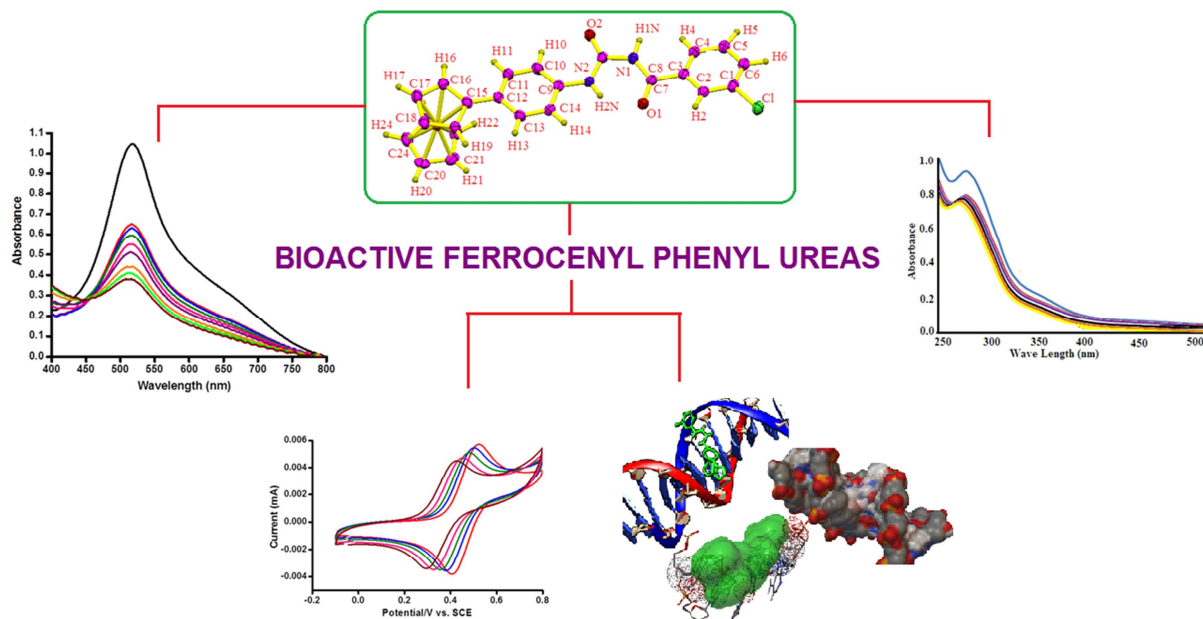
Received Date: 3 April 2015

Revised Date: 5 August 2015

Accepted Date: 16 August 2015

Please cite this article as: F. Asghar, A. Badshah, R.A. Hussain, M. Sohail, K. Akbar, I.S. Butler, Synthesis, structural characterization, DNA binding and antioxidant potency of new ferrocene incorporated acyl ureas, *Journal of Organometallic Chemistry* (2015), doi: 10.1016/j.jorganchem.2015.08.010.

This is a PDF file of an unedited manuscript that has been accepted for publication. As a service to our customers we are providing this early version of the manuscript. The manuscript will undergo copyediting, typesetting, and review of the resulting proof before it is published in its final form. Please note that during the production process errors may be discovered which could affect the content, and all legal disclaimers that apply to the journal pertain.



## Synthesis, structural characterization, DNA binding and antioxidant potency of new ferrocene incorporated acyl ureas

Faiza Asghar<sup>a,b</sup>, Amin Badshah<sup>a\*</sup>, Raja Azadar Hussain<sup>a</sup>, Manzar Sohail<sup>c</sup>, Kamran Akbar<sup>a</sup>, Ian Sydney Butler<sup>b</sup>

a\*. Corresponding Author: Coordination Chemistry Laboratory, Department of Chemistry, Quaid-i-Azam University (45320) Islamabad, Pakistan. aminbadshah@yahoo.com

a. Coordination Chemistry Laboratory, Department of Chemistry, Quaid-i-Azam University (45320) Islamabad, Pakistan.

b. Department of Chemistry, McGill University, Montreal, QC, Canada H3A 2K6

c. Faculty of Science, Health, Education and Engineering ML12, University of the Sunshine Coast, Australia.

### Abstract:

In this article, we have reported the synthesis of three new ferrocene incorporated ureas namely; 1-(4-Chlorobenzoyl)-3-(4-ferrocenylphenyl)urea (P4Cl), 1-(3-Chlorobenzoyl)-3-(4-ferrocenylphenyl)urea (P3Cl) and 1-(2-Chlorobenzoyl)-3-(4-ferrocenylphenyl)urea (P2Cl). All new compounds were unambiguously characterized by common analytical techniques (NMR, FT-IR, AAS, CHNS and molecular docking). Furthermore, single crystal XRD analysis was done for 1-(3-Chlorobenzoyl)-3-(4-ferrocenylphenyl)urea. DNA binding is a pre-requisite for a compound to be used as an antitumor agent. The DNA binding study was done by cyclic voltammetry, UV-vis spectroscopy and viscometry. The drug-DNA binding constant was found to vary in the sequence:  $K_{P2Cl} (6.056 \times 10^4 M^{-1}) > K_{P4Cl} (5.713 \times 10^4 M^{-1}) > K_{P3Cl} (4.631 \times 10^4 M^{-1})$ . Diffusion coefficient of the drug-DNA adduct for all the compounds is lower than the free drug, indicating that drug-DNA adduct is of higher molecular weight and slow diffusing as compared to the free drug. Small binding site size of 0.440 (P3Cl), 0.585 (P4Cl) and 0.673 (P2Cl) base pairs is consistent with electrostatic interaction. All the compounds exhibited good antioxidant activities with  $IC_{50}$  values of 82, 136 and 54  $\mu M$  for P4Cl, P3Cl and P2Cl respectively, against DPPH.

Key words: DNA binding constant, diffusion coefficients, desulphurization, binding site size.

### 1. Introduction

In the area of tumor treatment, interaction of different possible drugs with DNA is improving day by day. DNA is an important biological molecule which contains all the genetic

information for the proper functions of the cells. Drug-DNA interactions may be categorized as: a) electrostatic, b) groove binding and c) intercalation. It is believed that if we are able to have a check on the uncontrolled proliferation of the cells through any of the above mentioned interactions with DNA then we will be able to control the cancer [1]. Cisplatin is a potent antineoplastic agent but has some negative side effects. In search of the compounds which should be active like cisplatin but with minimal or no side effects, different classes of the compounds have been under investigation. In this struggle tremendous attention has been given to the ferrocene and its derivatives. Ferrocene [2], nitrophenyl ferrocene [3], antimony derivatives of ferrocene [1] and thiourea [4] and selenourea derivatives of ferrocene [5-7] have been evaluated for their interactions with DNA. It has been observed that almost all the derivatives of ferrocene have higher drug-DNA binding constant than simple positively charged ferrocene moiety ( $3.45 \times 10^2 \text{ M}^{-1}$ ) although when these derivatives are not coupled with ferrocene then they are themselves less active for DNA. Therefore it is need of the time to explore such derivatives which may orient themselves with DNA in such a way that they can control the proliferation of infected cells. Generally ferrocene derivatives interact electrostatically with DNA but partial intercalation also have been reported [4]. Use of ferrocene moiety has multifold advantages in term of its anticancer, antibiotic and antimalarial activities [8]. Moreover, it enhances the lipophilicity and is a beautiful electrochemical marker during cyclic voltammetric studies. Without the use of ferrocene it is difficult to study the DNA binding of ureas with cyclic voltammetry as their electrochemical signals are very weak. Different techniques (UV-vis, fluorescence, luminescence, laser light scattering) have been used for the evaluation of drug-DNA binding constant but electrochemical methods are cost effective, highly sensitive and have fast detection [2].

On the other hand, ureas have huge applications as antiproliferative agents [9], anticancer agents (renal cancer, colon cancer, lungs cancer, prostate cancer and breast cancer) [10], anti platelets aggregatives, antifungal and antibacterial agents [11]. Inspired from the applications of ferrocenes and ureas separately we have combined them in a new class i.e. ferrocene incorporated ureas. We have presented in this paper, synthesis, structural characterization and DNA binding study of three new ferrocene based ureas. Single crystal X-ray structure for P3Cl is also provided. All the compounds have been completely characterized with multinuclear ( $^1\text{H}$  and  $^{13}\text{C}$ ) NMR, FT-IR, elemental analysis and atomic absorption spectrophotometry (AAS). Drug-

DNA binding has been determined with cyclic voltammetry (CV) and mode of interaction has further been confirmed with UV-vis spectroscopy, molecular docking and viscometry. We have also reported their antioxidant activity in addition.

## 2. Experimental

### 2.1 Materials and Methods

Melting points were determined in a capillary tube using electro-thermal melting point apparatus model MP-D Mitamura Riken Kogyo (Japan). Infrared spectra were taken on Thermoscientific NICOLET 6700 FTIR.  $^1\text{H}$  and  $^{13}\text{C}$  NMR measurements were recorded on a Bruker AV500 MHz spectrometer in DMSO.  $\text{Si}(\text{CH}_3)_4$  was used as internal reference. The elemental analysis were performed using a LECO-932 CHNS analyzer while the Fe concentrations were determined on an Atomic Absorption Spectrophotometer Perkin Elmer 2380.

Commercial salmon DNA was solubilized in doubly distilled water to prepare a stock solution of  $6 \times 10^{-4}$  M from which working concentrations of DNA were prepared. Concentration of stock solution was measured by UV absorbance at 260 nm using an epsilon value of  $6600 \text{ M}^{-1} \text{ cm}^{-1}$ . This DNA was protein free because  $A_{260}/A_{280} > 1.8$ .

Cyclic voltammetry was performed on Biologic SP-300 cyclic voltammeter running with EC-Lab Express V 5.40 software, Japan. Before every reading working electrode was polished with alumina powder and rinsed with distilled water. Analytical grade TBAP (Tertiarybutylammonium perchlorate) was used as supporting electrolyte and nitrogen gas (99.9 %) was purged through the mixture to avoid interference of oxygen.

The Ubbelohde viscometer was used for viscosity measurements at room temperature ( $25 \pm 1$  °C). Flow time was measured with a digital stopwatch. Flow time measurements were made in triplicate for the measurement of average flow time. Data were presented as relative specific viscosity ( $\eta/\eta_0$ ), vs. binding ratio ( $[\text{Drug}]/[\text{DNA}]$ ) where  $\eta$  is the viscosity of DNA in the presence of complex and  $\eta_0$  is the viscosity of DNA alone.

Docking studies were carried out using Autodock (Version 4.2) docking software [12]. Structure of B-DNA dodecamer  $\text{d}(\text{CGCGAATTCGCG})_2$  (1BNA) was taken from

protein data bank (PDB) [13] while Crystallographic Information File of P3Cl was used as ligand for subsequent docking. Essential hydrogen atoms and Gasteiger charges were added with the aid of Auto-Dock tools (ADT). The grid size was set to 64, 64 and 116 along the x, y and z-axes respectively. The center of the grid was set to 14.98, 20.976 and 8.807. After DNA was enclosed in the grid defined with 0.375 Å spacing, the grid map was calculated using the AutoGrid program. Docking to macromolecule was performed using an empirical free energy function and Lamarckian Genetic Algorithm, with an initial population of 50 randomly placed individuals, a maximum number of  $2 \times 10^5$  energy evaluations, a mutation rate of 0.02, and a crossover rate of 0.80 were given. P3Cl molecule was allowed to move within a specified region to achieve the lowest energy conformation while B-DNA dodecamer was kept rigid during docking.

The reducing abilities of P4Cl, P3Cl and P2Cl were determined with the help of 1,1-diphenyl-2-picrylhydrazyl in DMSO to produce 1,1-diphenyl-2-picrylhydrazine. Decrease in the absorption of 1,1-diphenyl-2-picrylhydrazyl (DPPH) was monitored to calculate % age scavenging according to the following formula [7, 14]:

$$\text{Scavenging Activity (\%)} = A_0 - A / A_0 \times 100$$

Where  $A_0$  is the absorbance of free DPPH and A is the absorption of DPPH-drug mixture with increasing concentration of drug. To a solution of DPPH (3.9 mg of DPPH in 100 mL DMSO) were added the increasing concentrations (27  $\mu\text{M}$ ) of drug. The decrease in absorption of DPPH was monitored after 30 minutes at wavelength of 517 nm with the help of spectrophotometer. All the readings were taken in triplicate and average of all the readings were used.

Ferrocene, Paranitro aniline, sodium nitrite, diethyl ether, acetone, DMSO, Pd-charcoal, hydrazine, KSCN, NaOH,  $\text{HgCl}_2$  and acid chlorides such as 4-chlorobenzoyl chloride, 3-chlorobenzoyl chloride and 2-chlorobenzoyl chloride were obtained from commercial sources (Sigma Aldrich/Fluka) and used as received. Para ferrocenyl aniline and ferrocene incorporated N, N-disubstituted thioureas were synthesized by a procedure reported by our group previously (Part 1 Scheme 1) [4, 15].

## 2.2 General procedure for synthesis of ferrocene incorporated ureas

To the solution of ferrocene incorporated N, N-disubstituted thioureas in 20 ml DMF, mercuric chloride was introduced in 1:1 molar ratio. The reaction mixture was stirred for 30 min,

afterwards 3 ml of 100 mM NaOH<sub>(aq)</sub> was added dropwise with constant magnetic stirring and the suspension was allowed to reflux for about 8 hrs. Progress of the reaction was examined by thin layer chromatography (TLC). On completion of the reaction black precipitates of HgS were filtered off and the filtrate was then poured into ice cold water and stirred well in order to remove water soluble impurities. Solid product was separated by filtration, washed with deionized water and recrystallized from ethanol (Scheme 1).

### 2.2.1 1-(4-Chlorobenzoyl)-3-(4-ferrocenylphenyl)urea (P4C1)

Quantities used were 0.5 g (0.00105 mol) 1-(4-Chlorobenzoyl)-3-(4-ferrocenylphenyl) thiourea, 0.29 g (0.00105 mol) HgCl<sub>2</sub> and 3 ml of 100 mM NaOH<sub>(aq)</sub>. Yield 74 %; Yellow solid; m.p. 210 °C; FT-IR (powder, cm<sup>-1</sup>): 3232 (N-H), 3035 (C-H<sub>aromatic</sub>), 1696 (C=O), 1474-1586 (C=C), 484 (Fe-Cp); <sup>1</sup>H NMR (500 MHz, DMSO-d<sup>6</sup>, ppm) δ 11.20 (s, 1H, NH), 10.81 (s, 1H, NH), 7.94 (d, 2H, ArH), 7.38 (d, 4H, ArH), 7.09 (d, 2H, ArH), 4.70 (s, 2H, C<sub>5</sub>H<sub>4</sub>), 4.29 (s, 2H, C<sub>5</sub>H<sub>4</sub>), 4.02 (s, 5H, C<sub>5</sub>H<sub>5</sub>); <sup>13</sup>C NMR (125.81 MHz, DMSO-d<sup>6</sup>, ppm) δ 167.2, 160.5, 137.9, 132.9, 131.1, 130.8, 129.1, 128.9, 127.6, 122.4, 84.9, 69.7, 69.2, 66.4; Elemental Analysis Calc. (%) for C<sub>24</sub>H<sub>19</sub>ClFeN<sub>2</sub>O<sub>2</sub>: C, 62.83; H, 4.18; N, 6.10; Fe, 12.17. Found (%): C, 62.78; H, 4.12; N, 6.16; Fe, 12.26.

### 2.2.2 1-(3-chlorobenzoyl)-3-(4-ferrocenylphenyl)urea (P3Cl)

Quantities used were 0.5 g (0.00105 mol) 1-(3-Chlorobenzoyl)-3-(4-ferrocenylphenyl) thiourea, 0.29 g (0.00105 mol) HgCl<sub>2</sub> and 3 ml of 100 mM NaOH<sub>(aq)</sub>. Yield 71 %; Brown solid; m.p. 185 °C (decompose); FT-IR (powder, cm<sup>-1</sup>): 3249 (N-H), 3082 (C-H<sub>aromatic</sub>), 1694 (C=O), 1458-1592 (C=C), 483 (Fe-Cp); <sup>1</sup>H NMR (500 MHz, DMSO-d<sup>6</sup>, ppm) δ 11.12 (s, 1H, NH), 10.68 (s, 1H, NH), 8.09 (s, 1H, ArH), 7.98 (d, 2H, *J* = 7.5 Hz, ArH), 7.74 (d, 2H, *J* = 8.0 Hz, ArH), 7.61-7.37 (m, 3H, ArH), 4.76 (s, 2H, C<sub>5</sub>H<sub>4</sub>), 4.33 (s, 2H, C<sub>5</sub>H<sub>4</sub>), 4.08 (s, 5H, C<sub>5</sub>H<sub>5</sub>); <sup>13</sup>C NMR (125.81 MHz, DMSO-d<sup>6</sup>, ppm) δ 167.8, 161.3, 135.8, 134.4, 133.8, 131.0, 128.6, 127.5, 126.8, 120.4, 86.8, 69.8, 69.2, 66.5; Elemental Analysis Calc. (%) for C<sub>24</sub>H<sub>19</sub>ClFeN<sub>2</sub>O<sub>2</sub>: C, 62.83; H, 4.18; N, 6.10; Fe, 12.17. Found (%): C, 62.86; H, 4.14; N, 6.13; Fe, 12.19.

### 2.2.3 1-(2-Chlorobenzoyl)-3-(4-ferrocenylphenyl)urea (P2C1)

Quantities used were 0.5 g (0.00105 mol) 1-(2-Chlorobenzoyl)-3-(4-ferrocenylphenyl) thiourea, 0.29 g (0.00105 mol)  $\text{HgCl}_2$  and 3 ml of 100 mM  $\text{NaOH}_{(\text{aq})}$ . Yield 66 %; Orange solid; m.p. 198 °C; FT-IR (powder,  $\text{cm}^{-1}$ ): 3243 (N-H), 3089 ( $\text{C-H}_{\text{aromatic}}$ ), 1688 (C=O), 1471-1600 (C=C), 482 (Fe-Cp);  $^1\text{H}$  NMR (500 MHz,  $\text{DMSO-d}^6$ , ppm)  $\delta$  11.21 (s, 1H, NH), 10.41 (s, 1H, NH), 7.63-7.46 (m, 8H, ArH), 4.77 (s, 2H,  $\text{C}_5\text{H}_4$ ), 4.33 (s, 2H,  $\text{C}_5\text{H}_4$ ), 4.03 (s, 5H,  $\text{C}_5\text{H}_5$ );  $^{13}\text{C}$  NMR (125.81 MHz,  $\text{DMSO-d}^6$ , ppm)  $\delta$  171.2, 160.6, 135.8, 135.0, 132.4, 130.2, 129.6, 127.7, 126.8, 120.4, 83.4, 69.8, 69.2, 66.5; Elemental Analysis Cal. (%) for  $\text{C}_{24}\text{H}_{19}\text{ClFeN}_2\text{O}_2$ : C, 62.83; H, 4.18; N, 6.10; Fe, 12.17. Found (%): C, 62.79; H, 4.21; N, 6.08; Fe, 12.20.

### 3. Results and Discussion

#### 3.1 Chemistry

Treatment of ferrocene based thioureas with alkaline mercuric chloride in DMF yielded the respective ureas. The targeted compounds were synthesized by the replacement of sulfur with oxygen, [16] in the presence of alkaline  $\text{Hg}^{2+}$  as sulfur capturing agent that yielded ureas in good yield. NaOH was used as an alkali which provides  $\text{OH}^-$  anion that attacks on thio-carbon of thiourea. The proposed mechanism similar to that of guanylation is shown in Scheme 3 [17].

#### 3.2 Spectroscopic Analysis

In the FT-IR spectra of synthesized compounds the two  $-\text{NH}$  protons gave a broad signal between 3250-3228  $\text{cm}^{-1}$  owing to intra and intermolecular hydrogen bonding. The stretch due to Aromatic-H's was evident just above 3000  $\text{cm}^{-1}$ , while the carbonyl group appeared as an intense band at 1696-1688  $\text{cm}^{-1}$ . All the compounds (P4Cl, P3Cl and P2Cl) have basically three types of protons i.e. protons of ferrocene, protons of  $-\text{NH}$  and aromatic protons. In the  $^1\text{H}$  NMR spectra, all the compounds displayed two singlets for the two  $-\text{NH}$  protons.  $-\text{NH}$  proton which is present between two carbonyl carbons is maximum deshielded and provides a singlet at ~11 ppm. The second  $-\text{NH}$  which is attached to the phenyl ring is comparatively less deshielded, therefore it appears as a singlet at ~10 ppm. Five protons of unsubstituted cyclopentadiene (Cp) ring of ferrocene yielded an intense signal at ~4 ppm and substituted Cp provided two singlets downfield from the singlet of unsubstituted Cp ring. Aromatic protons were visible between 8-7 ppm. In  $^{13}\text{C}$  NMR maximum downfield carbon was between the two  $-\text{NH}$  groups with a value of 171-167 ppm. The other carbonyl carbon appeared at ~161 ppm because it was comparatively

less deshielded. The Aromatic-C appears between 143-117 ppm. Unsubstituted Cp carbons of ferrocene gave an intense singlet whereas substituted Cp provided three peaks i.e. the ipso carbon appeared between 87-83 ppm and the other two signals were apparent between 70-66 ppm.

Elemental analysis of all the compounds showed that the calculated and found values for carbon, hydrogen, nitrogen and iron are in close agreement with each other. The carbon, hydrogen and nitrogen percentages were determined with a CHNS analyser and that of Fe by AAS.

### 3.3 Crystallography

Diffraction data of P3Cl were collected at 100 (2) K on beamline MX1 at the Australian Synchrotron ( $\lambda = 0.71703 \text{ \AA}$ ) [18]. The data reduction and indexing of diffraction pattern was performed by XDS software [19]. The structures were solved by direct methods and refined by full-matrix least squares against  $F^2$  of data using SHELXL97 (Sheldrick, 1997) software. All non-hydrogen atoms were refined with anisotropic displacement parameters. Basic crystal data and description of diffraction experiment are given in Table 1. ORTEP of P3Cl is given in Figure 1a whereas selected bond lengths and bond angles have been given in Table 2. The structure reveals that the phenyl ring attached with Cp of ferrocene is not exactly in plane with Cp moiety and is tilted at an angle of  $30^\circ$  whereas terminal chloro substitutes phenyl ring is at an angle of  $53.37^\circ$  from the plane of Cp moiety. Hydrogens of the ferrocene are staggered and O (1) has an intramolecular hydrogen bond with the H (2) whereas intermolecular hydrogen bond is between O (2) of one molecule and H (1) of the other molecule (Figure 1b). A partial interaction between H (4) and O (2) is also visible in the structure (Figure 1b). Packing of the molecule reveals that it exists as a monomer and ferrocene moieties of two neighboring molecules are at a maximum distance from each other with trans orientation (Figure 1c).

### 3.4 Cyclic Voltammetry

Cyclic voltammetric studies were carried out with a setup having three electrodes system i.e. working (platinum disc electrode with a geometric area of  $0.071 \text{ cm}^2\text{s}^{-1}$ ), reference (saturated calomel electrode i.e. SCE) and auxiliary electrodes (platinum electrode with geometric area much greater than working electrode). Changes in the peak current provided information about

DNA binding constant whereas the variation in the peak potential were useful for the determination of mode of interaction of drug with DNA. Drug-DNA binding constant was determined with the help of following equation [20]:

$$\log (1/[DNA]) = \log K + \log (I/I_0 - I) \quad \text{Eq 1}$$

Where K is the binding constant and  $I_0$  and I are the peak currents of free drug and DNA bound drug respectively. Binding site size was calculated with the help of following equation [21]:

$$C_b/C_f = K[\text{free base pairs}]/s \quad \text{Eq 2}$$

Where s is the binding site size in terms of base pair, K is the binding constant,  $C_b$  is the concentration of free species and  $C_f$  represents concentration of drug-DNA bound species. If we consider the concentration of DNA in terms of nucleotide phosphate, then the concentration of DNA base pairs will be equal to  $[DNA]/2$  and Eq 2 will be written as:

$$C_b/C_f = K[DNA]/2s \quad \text{Eq 3}$$

and the value of  $C_b/C_f$  is equal [19] to  $(I_0 - I/I)$  which are the values of experimental peak currents. The diffusion coefficient of free drug and DNA-bound drug provides best information about the molecular mass of drug-DNA adduct. Following form of Randles-Sevcik Equation [22, 23] was used for the values of diffusion coefficients:

$$I_{pa} = 2.99 \times 10^5 n^{3/2} A C_o^* D_o^{1/2} \nu^{1/2} \quad \text{Eq 4}$$

Where  $I_{pa}$  is the anodic peak current  $C_o^*$  is the reductant's concentration in  $\text{molcm}^{-3}$ , A is the geometric area of the electrode in  $\text{cm}^2$ , n is the number of electrons involved in the process,  $D_o$  is the diffusion coefficient in  $\text{cm}^2\text{s}^{-1}$ .

Consistency of voltage at different scan rates by a plot of current (mA) vs. potentials (E/V vs. SCE) for all the three compounds i.e P3Cl, P4Cl and P2Cl (Figure 2a) favours 100 % reversible electrochemical process. P3Cl provides a couple of well defined redox peaks with an oxidation maxima at 0.522 V and a reduction maxima at 0.404 V. For the calculation of drug-DNA binding constant, changes in oxidation peak were monitored with successive addition of 2-8  $\mu\text{M}$  DNA solutions (Figure 2b). With the addition of 2  $\mu\text{M}$  DNA in cyclic voltammetric cell there is a 26 mV shift towards the negative potential with a decrease in the peak current. This

negative shift in the peak potential conforms electrostatic mode of interaction of positively charged P3Cl with a negatively charged phosphate backbone of the DNA. Decrease in peak current with successive addition of DNA was used to determine the P3Cl-DNA binding constant of  $4.631 \times 10^4 \text{ M}^{-1}$  with the help of Eq 1 (Figure 2d). This value of binding constant is far better than protonated ferrocene ( $3.45 \times 10^2 \text{ M}^{-1}$ ) and is comparable with many of the recently reported ferrocene derivatives (Scheme 2) which shows that urea moiety is playing its part in the enhancement of binding constant. The diffusion coefficient of P3Cl-DNA is  $6.47 \times 10^{-7} \text{ cm}^2\text{s}^{-1}$  which is far less than the diffusion coefficient of free P3Cl ( $7.44 \times 10^{-7} \text{ cm}^2\text{s}^{-1}$ ). This indicates that the drug-DNA adduct is of higher molecular mass and slow diffusing as compared to the free drug (Figure 2c). Binding site of 0.440 bp was calculated with the help of Eq. 2 (Figure 2e). This small value of binding site size is an evidence for electrostatic mode of interaction.

P4Cl also provides a couple of well defined redox peaks in the potential region of -0.2–0.9 V which provided the DNA binding constant of  $5.713 \times 10^4 \text{ M}^{-1}$  (Figure 3a). A negative shift in potential and a decrease in peak current on successive addition of DNA suggests an electrostatic interaction of P4Cl with DNA. P4Cl-DNA adduct has a lower diffusion coefficient ( $4.42 \times 10^{-7} \text{ cm}^2\text{s}^{-1}$ ) than the free P4Cl ( $6.55 \times 10^{-7} \text{ cm}^2\text{s}^{-1}$ ), which is indicative for the formation of slow diffusing P4Cl-DNA adduct.

P2Cl also behaves similar to P3Cl and P4Cl with binding constant of  $6.056 \times 10^4 \text{ M}^{-1}$ , which is less than P3Cl and P4Cl. As mentioned above P2Cl-DNA adduct has lower diffusion coefficient ( $2.80 \times 10^{-7} \text{ cm}^2\text{s}^{-1}$ ) than free P2Cl ( $5.47 \times 10^{-7} \text{ cm}^2\text{s}^{-1}$ ). P2Cl also binds electrostatically with DNA (Figure 3b). Binding site size varies in following order: P2Cl (0.673 bp) > P4Cl (0.585 bp) > P3Cl (0.440 bp), such small values of  $s$  confirms electrostatic interaction.

### 3.5 UV-vis Spectroscopy

The results obtained from CV were equally supported by UV-vis spectroscopy in which a prominent hypochromism and a slight blue shift of the drug-DNA adducts relative to the free drug confirms the electrostatic interactions (Figure 4a). A DNA binding constant of  $5.004 \times 10^4 \text{ M}^{-1}$  for P3Cl is in very close agreement with the values obtained from CV (Figure 4b) [6].

### 3.6 Viscometry

Mode of interaction was further confirmed with the help of viscometry as well. Figure 5 shows representative plot of relative viscosity ( $\eta/\eta_0$ ) against [P3Cl]/[DNA] concentrations. P3Cl shows a decrease in relative viscosity with increasing binding ratio which is a characteristic for electrostatic interactions [6]. DNA binding constant of  $7.8752 \times 10^4 \text{ M}^{-1}$  is in agreement with the values of binding constant determined with CV.

### 3.7 Molecular Docking

Figure 6a shows the representative docked conformation of P3Cl with DNA, having lowest binding energy, suggested by Autodock while Figure 6b represents the surface view of the same docked conformation. It is evident from Figure 6b that ferrocenyl moiety of the docked P3Cl is in close contact with oxygen attached to sugar-phosphate backbone of DNA which in turns suggest electrostatic force of interaction between Iron and oxygen of sugar-phosphate backbone. Figure 6c shows the close-up view of the atoms of DNA which are interacting with the surface of P3Cl and it can be seen that oxygen of sugars-phosphate back bone, present between deoxyadenosine (DA)-18 and DA17, is interacting with ferrocenyl moiety, electrostatically. It can also be seen that, there is also hydrogen bond present between one of the oxygen of P3Cl and hydrogen attached to nitrogen of DA5 [6, 24, 25].

### 3.8 DPPH Scavenging activity

DPPH provides a strong absorption band at 517 nm due to its odd electron. When any antioxidant reacts with DPPH it produces 1,1-diphenyl-2-picrylhydrazine. As a result the band intensity of DPPH decreases. This changes the color of DPPH and a corresponding decrease in the absorption. Figure 7 shows a representative plot of absorbance versus wavelength for P3Cl.  $\text{IC}_{50}$  values of 82, 136 and 54  $\mu\text{M}$  were determined for P3Cl, P4Cl and P2Cl respectively.

## 4. Conclusions

Synthesis of anticipated compounds was accomplished as a result of deprotection of ferrocene incorporated thioureas to corresponding oxo analogue. Characterization by different techniques confirms the formation of targeted ureas. Synthesized ferrocene incorporated ureas show electrostatic mode of interaction with DNA and a decent binding constant value. Their antioxidant activity is also reasonable with reference to ascorbic acid.

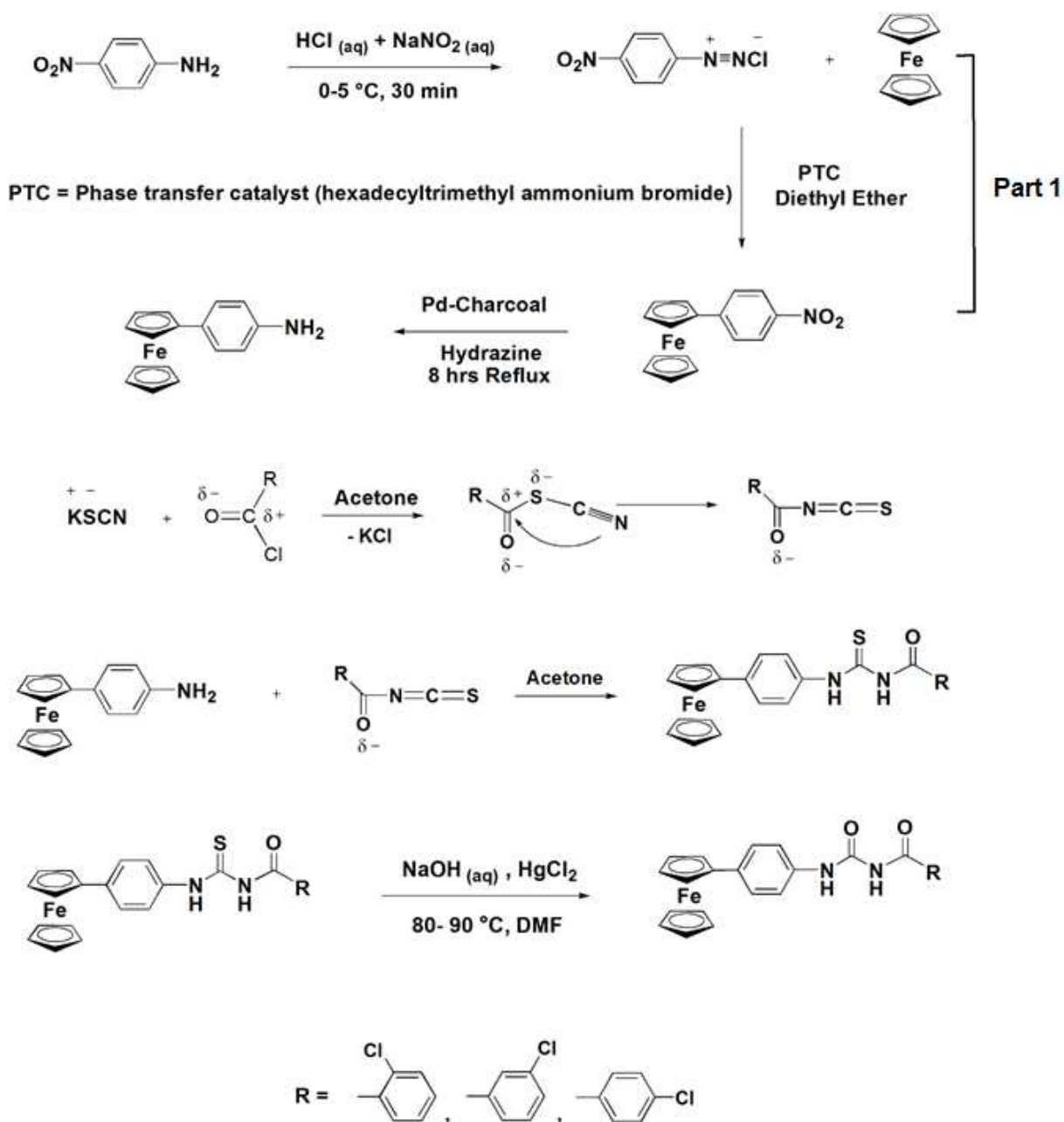
## Acknowledgements

Faiza Asghar is highly obliged to the Higher Education Commission (HEC) of Pakistan for providing scholarship under the program 5000 Indigenous PhD Scholarships at Quaid-i-Azam University in Islamabad and for a 6-month scholarship under the International Research Support Initiative program (IRSIP) as a Graduate Research Trainee in the Department of Chemistry, McGill University, Montreal, Quebec, Canada.

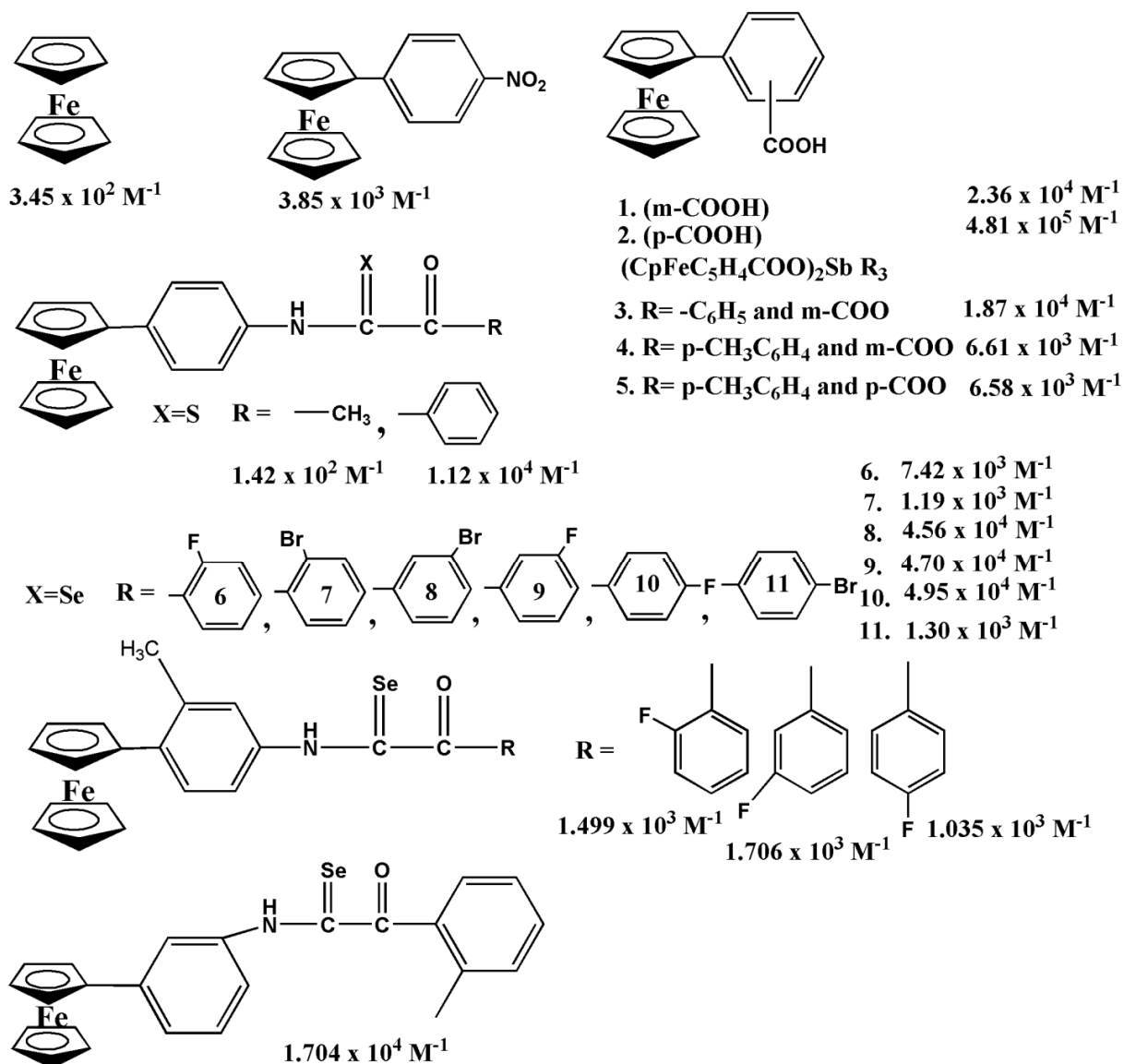
## References

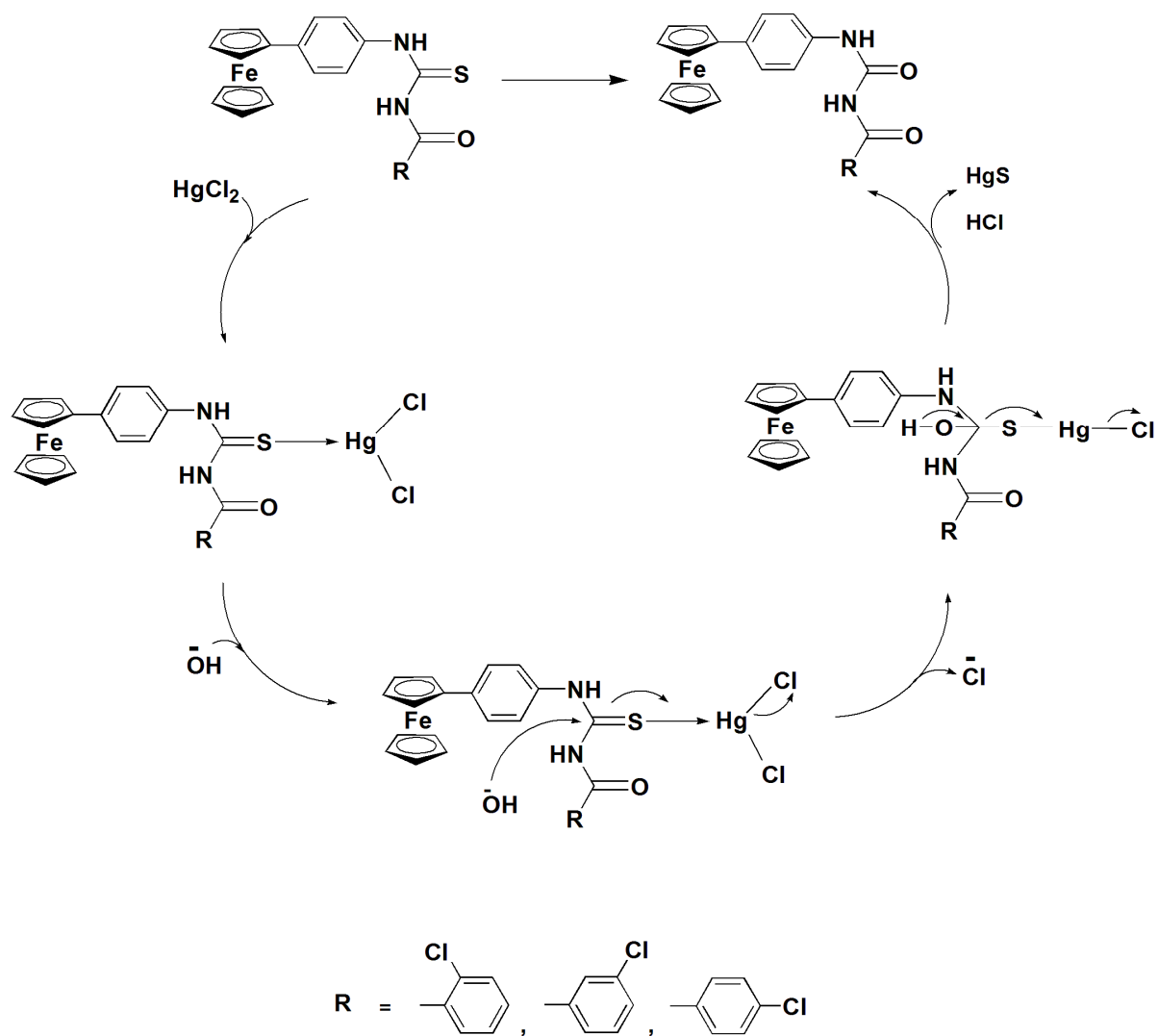
- [1] F. Asghar, A. Badshah, A. Shah, M.K. Rauf, M.I. Ali, M.N. Tahir, E. Nosheen, R. Zia ur, R. Qureshi, *J. Organomet. Chem.* 717 (2012) 1-8.
- [2] A. Shah, R. Qureshi, N.K. Janjua, S. Haque, S. Ahmad, *Anal. Sci.* 24 (2008) 1437-1441.
- [3] A. Shah, M. Zaheer, R. Qureshi, Z. Akhter, M. Faizan Nazar, *Spectrochim. Acta, Part A: Molecular and Biomolecular Spectroscopy*, 75 (2010) 1082-1087.
- [4] B. Lal, A. Badshah, A.A. Altaf, M.N. Tahir, S. Ullah, F. Huq, *Dalton Trans.* 41 (2012) 14643-14650.
- [5] R.A. Hussain, A. Badshah, M. Sohail, B. Lal, K. Akbar, *J. Mol. Struct.* 1048 (2013) 367-374.
- [6] R.A. Hussain, A. Badshah, M.N. Tahir, B. Lal, I.A. Khan, *Aust. J. Chem.* 66 (2013) 626-634.
- [7] R.A. Hussain, A. Badshah, M. Sohail, B. Lal, A.A. Altaf, *Inorg. Chim. Acta.* 402 (2013) 133-139.
- [8] B. Lal, A. Badshah, A.A. Altaf, N. Khan, S. Ullah, *Appl. Organomet. Chem.* 25 (2011) 843-855.
- [9] M. Radić Stojković, S. Marczi, L. Glavaš-Obrovac, I. Piantanida, *Eur. J. Med. Chem.* 45 (2010) 3281-3292.
- [10] E.L. Luzina, A.V. Popov, *Eur. J. Med. Chem.* 45 (2010) 5507-5512.
- [11] P. Ventosa-Andrés, Á.M. Valdivielso, I. Pappos, M.T. García-López, N.E. Tsopanoglou, R. Herranz, *Eur. J. Med. Chem.* 58 (2012) 98-111.
- [12] G.M. Morris, R. Huey, W. Lindstrom, M.F. Sanner, R.K. Belew, D.S. Goodsell, A.J. Olson, *J. Comput. Chem.* 30 (2009) 2785-2791.
- [13] H.R. Drew, R.M. Wing, T. Takano, C. Broka, S. Tanaka, K. Itakura, R.E. Dickerson, *Proceedings of the National Academy of Sciences*, 78 (1981) 2179-2183.
- [14] (a) S. Zouari, M. Ketata, N. Boudhrioua, E. Ammar. *Ind. Crop Prod.* 41 (2013) 172-178;

- (b) A. Choudhary, R. Sharma, M. Nagar, M. Mohsin, H. Meena, *J. Chil. Chem. Soc.* 56 (2011) 911–917.
- [15] S. Ali, A. Badshah, A.A. Ataf, B. Lal, K.M. Khan, *Med. Chem. Res.* 22(7) (2013) 3154-3159.
- [16] S.G. Davies, A.A. Mortlock, *Tetrahedron Lett.* 32 (1991) 4791.
- [17] C. Levallet, J. Lerpiniere, S.Y. Ko, *Tetrahedron.* 53 (1997) 5291.
- [18] *Analytical Chemistry*, 61 (1989) 1309A-1309A.
- [19] T.M. McPhillips, S.E. McPhillips, H.-J. Chiu, A.E. Cohen, A.M. Deacon, P.J. Ellis, E. Garman, A. Gonzalez, N.K. Sauter, R.P. Phizackerley, S.M. Soltis, P. Kuhn, *J. Synchrotron. Radiat.* 9 (2002) 401-406.
- [20] Q. Feng, N.-Q. Li, Y.-Y. Jiang, *Anal. Chim. Acta.* 344 (1997) 97-104.
- [21] M. Aslanoglu, G. Ayne, *Anal. Bioanal. Chem.* 380 (2004) 658-663.
- [22] A. Oliveira-Brett, J. Piedade, L. Silva, V. Diculescu, *Anal. Biochem.* 332 (2004) 321-329.
- [23] A.M. Oliveira-Brett, V. Diculescu, J.A.P. Piedade, *Bioelectrochemistry*, 55 (2002) 61-62.
- [24] V. Namasivayam, R. Günther, *Chem. Biol. Drug Des.* 70 (2007) 475-484.
- [25] F. Österberg, G.M. Morris, M.F. Sanner, A.J. Olson, D.S. Goodsell, *Proteins*, 46 (2002) 34-40.

**Scheme 1.** Synthetic scheme for ferrocene incorporated acyl ureas.

Scheme 2. Drug-DNA binding constants for ferrocene derivatives.



**Scheme 3.** Proposed mechanism for formation of ferrocene incorporated acyl ureas.

**Table 1.** Crystal Data of P3Cl.

	P3Cl
Empirical formula	C <sub>24</sub> H <sub>19</sub> ClFeN <sub>2</sub> O <sub>2</sub>
Formula weight	458.7
Temperature (K)	100 K
Wavelength Å	0.71073
a [Å]	7.987 (2)
b [Å]	9.9530 (12)
c [Å]	12.6520 (6)
$\alpha$ [deg]	81.935 (4)°
$\beta$ [deg]	89.228 (6)°
$\gamma$ [deg]	79.397 (15)°
Volume Å <sup>3</sup>	978.7 (3)
Crystal System	Triclinic
Space group	P-1
Z	2
Density (calculated)	1.557g/cm <sup>3</sup>
Index Ranges	-10<=h<=10, -12<=k<=12, -16<=l<=16
Absorption coefficient ( $\mu$ )	0.932 mm <sup>-1</sup>
F(000)	472
Goodness-of-fit on F <sup>2</sup> (S)	1.058
Largest diff. peak and hole	0.638 and -0.879 e.Å <sup>-3</sup>
Final R indices [I>2 $\sigma$ (I)]	R1 = 0.0520, wR2 = 0.1152
R indices (all data)	R1 = 0.0782, wR2 = 0.1379

**Table 2.** Selected Bond lengths [Å] and angles [°] for P3Cl.

C(8)-N(1)	1.406(4)
N(1)-H(1N)	0.88(4)
N(2)-H(2N)	0.83(5)
O(1)-C(7)-N(1)	123.0(3)
O(1)-C(7)-C(3)	121.3(3)
N(1)-C(7)-C(3)	115.7(3)
O(2)-C(8)-N(2)	125.2(3)
C(7)-N(1)-C(8)	128.5(3)
C(7)-N(1)-H(1N)	123(3)
C(8)-N(1)-H(1N)	108(3)
C(8)-N(2)-C(9)	126.2(3)
C(8)-N(2)-H(2N)	116(3)
C(9)-N(2)-H(2N)	118(3)
C(7)-N(1)-C(8)	128.5(3)

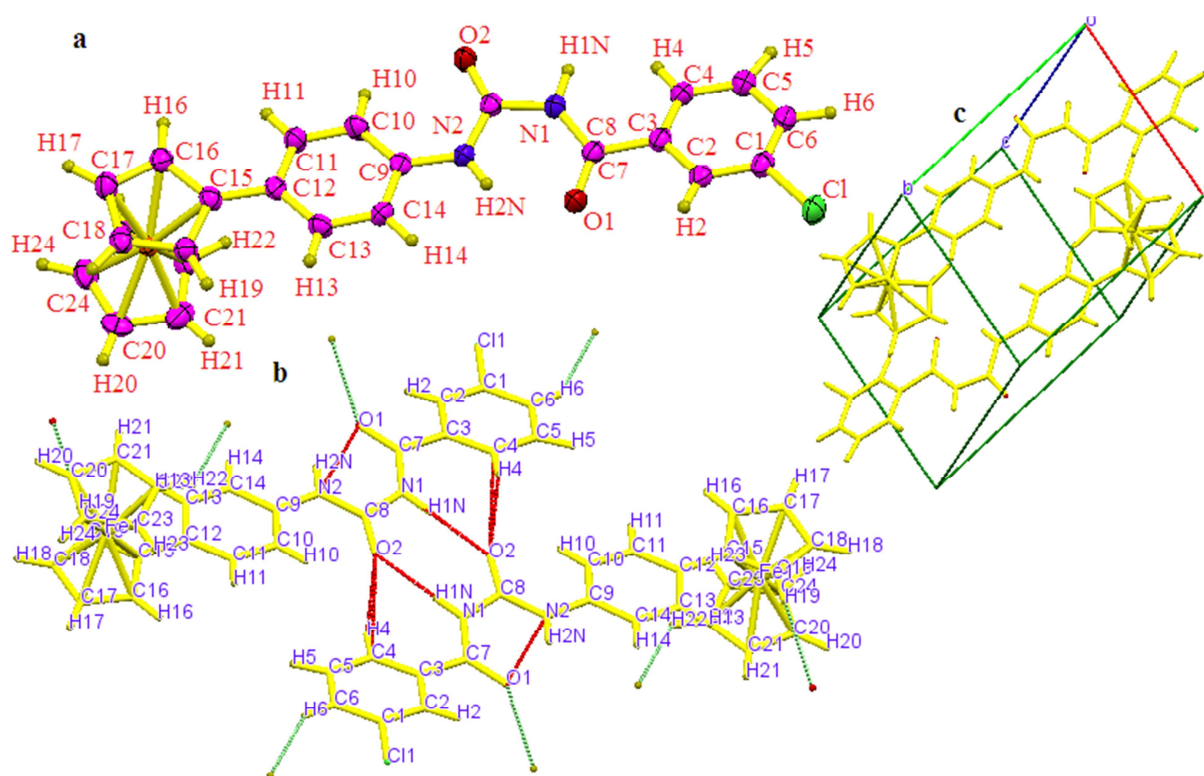


**Figure 1.** (a) Molecular diagram of P3Cl with ellipsoid displacement, non-hydrogen atoms represented by 30 % probability boundary spheres and hydrogen atoms are sphere of arbitrary size. (b) Hydrogen bonding in P3Cl. (c) Packing of P3Cl.

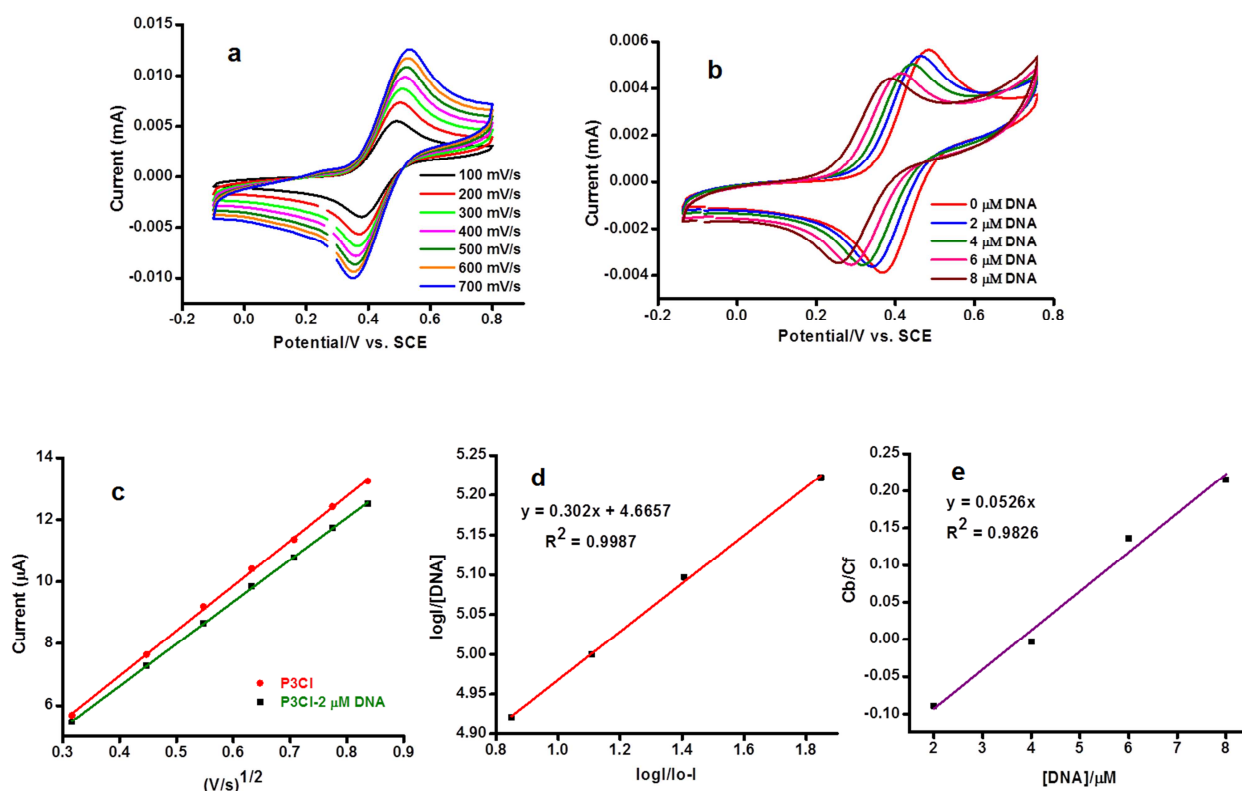


**Figure 2.** (a) Representative plots of Current vs. Potential/V (SCE) at different scan rates for P3Cl. (b) Cyclic voltammograms of 1 mM P3Cl with 1 mL of 0.5 M TBAP as supporting electrolyte in the absence and presence of 2-8  $\mu\text{M}$  DNA showing a decrease in  $I$  from  $I_0$  and a concentration dependent  $-ve$  shift in potential showing electrostatic interactions. (c) Representative plot of current vs.  $(V/s)^{1/2}$ , for the determination of diffusion coefficient of free P3Cl and P3Cl-2  $\mu\text{M}$  DNA. (d) Representative plot of  $\log(I/I_0 - I)$  vs.  $\log(1/[DNA])$  for determination of binding constant of P3Cl. (e) Plot of  $C_b/C_f$  vs.  $[DNA]/\mu\text{M}$  for determination of binding site size of 2-8  $\mu\text{M}$  DNA concentrations (P3Cl).

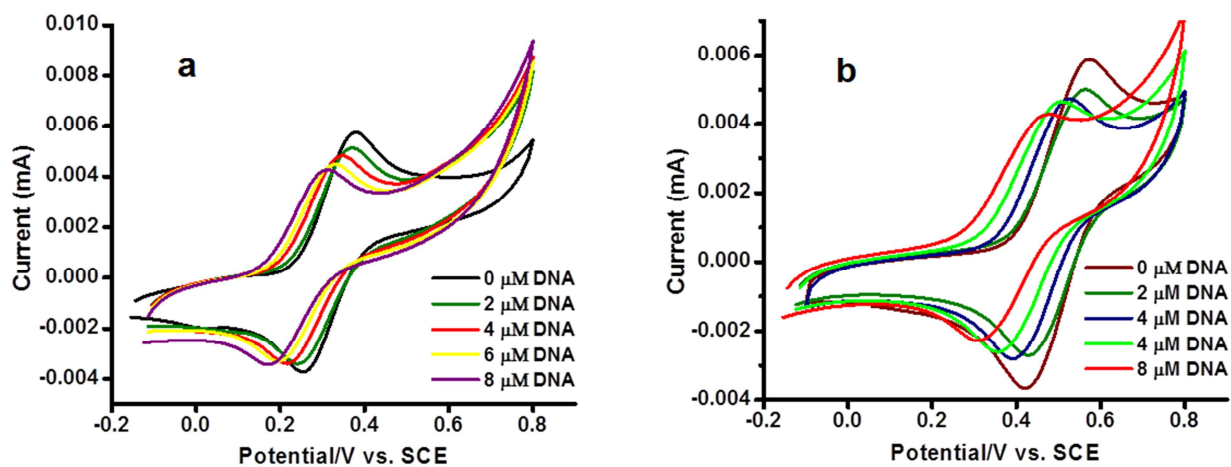


**Figure 3.** (a) Cyclic voltammograms of 1 mM P4Cl with 1 mL of 0.5 M TBAP as supporting electrolyte in the absence and presence of 2-8  $\mu\text{M}$  DNA showing a decrease in  $I$  from  $I_0$  and a concentration dependent  $-ve$  shift in potential showing electrostatic interactions. (b) Cyclic voltammograms of 1 mM P2Cl with 1 mL of 0.5 M TBAP as supporting electrolyte in the absence and presence of 2-8  $\mu\text{M}$  DNA.

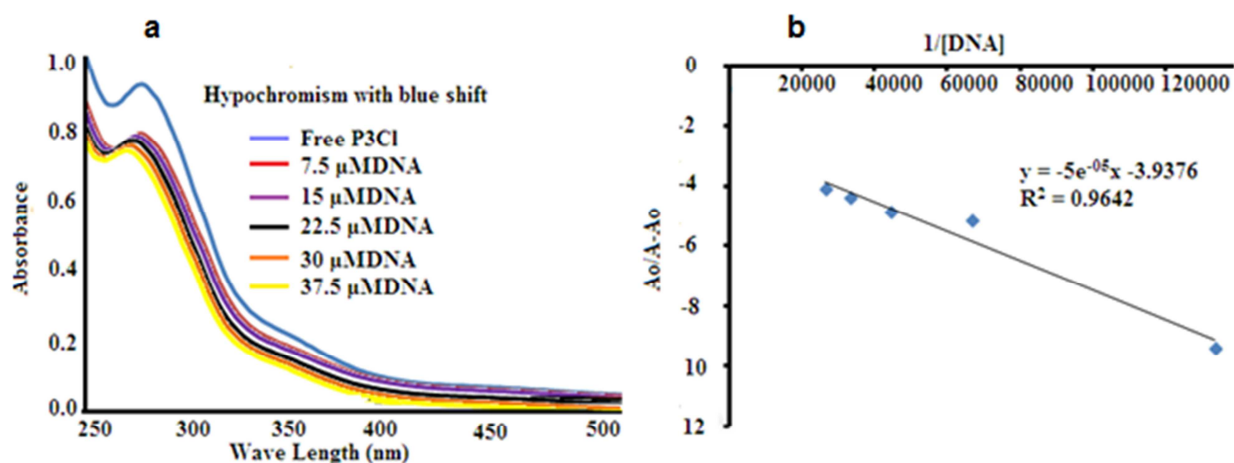


**Figure 4.** (a) Representative plots of absorbance versus wavelength of P3Cl with increasing concentration of DNA (7.5-37.5  $\mu\text{M}$ ). (b) Plot of  $A_0/A-A_0$  versus  $1/[\text{DNA}]$  for determination of DNA binding constant of P3Cl.

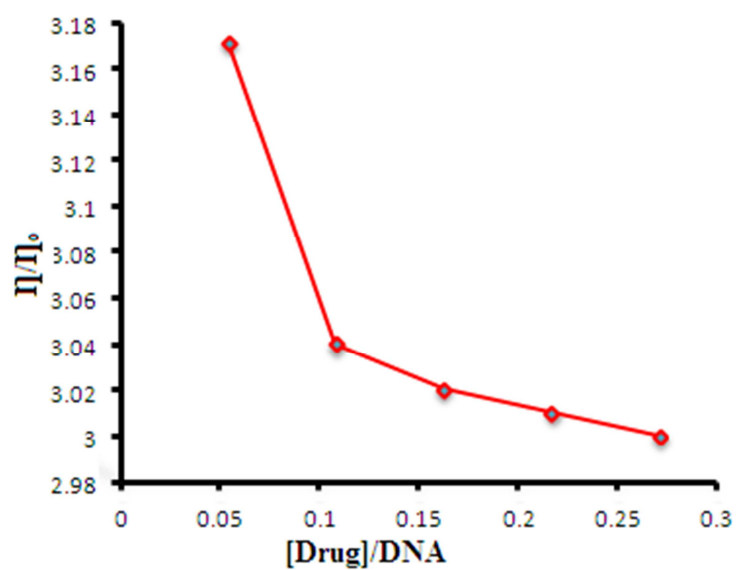


**Figure 5.** Representative plot of relative viscosity vs. [Drug]/[DNA] for determination of mode of interaction.

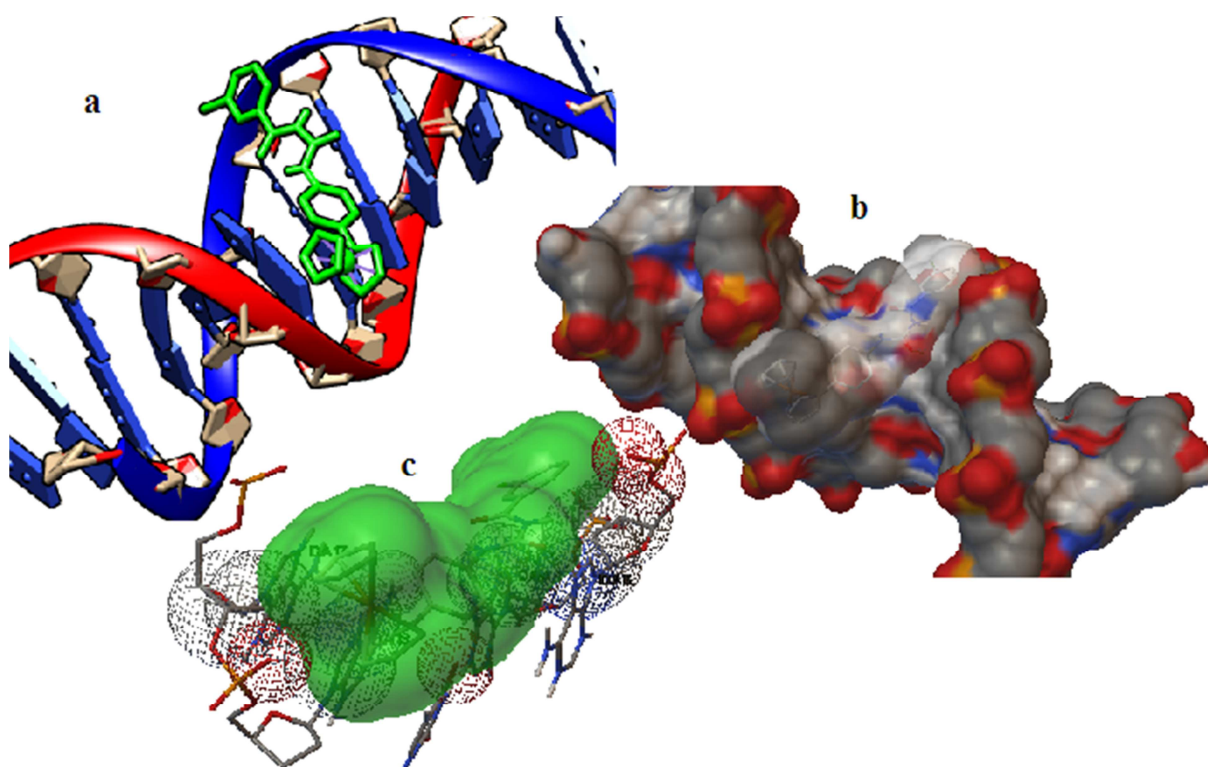


**Figure 6.** (a) Representative docked conformation of P3Cl with 1BNA, here P3Cl is in green color while 1BNA can be seen as ribbon structure. (b) Surface view of docked P3Cl with 1-BNA (Color code. Grey-carbon, Red- Oxygen, and Blue-Nitrogen). (c) Three-dimensional model showing interactions of P3Cl with the DNA.

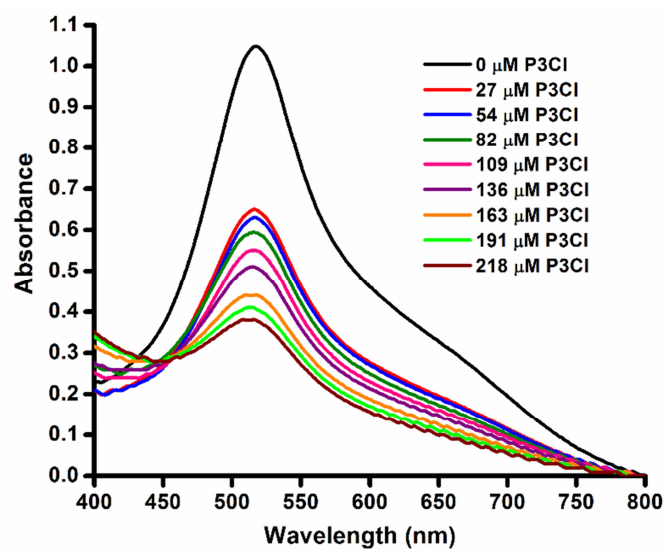


**Figure 7.** Representative plots of absorbance versus wavelength of P3Cl for DPPH scavenging activity.

- We have synthesized three new ferrocene incorporated acyl ureas.
- All the compounds were characterized by NMR, FT-IR, AAS, CHNS and single crystal XRD.
- CV, UV-vis spectroscopy, viscometry and molecular docking were used for DNA binding studies.
- IC<sub>50</sub> values of 82, 136 and 54  $\mu$ M for P4Cl, P3Cl and P2Cl respectively, were observed against DPPH.

Single crystal structure of ferrocene incorporated acyl ureas, their spectroscopic, electrochemical, antioxidant and molecular docking studies.

ACCEPTED MANUSCRIPT

**checkCIF/PLATON report**

Structure factors have been supplied for datablock(s) I

No syntax errors found. CIF dictionary Interpreting this report

**Datablock: I**

Bond precision: C-C = 0.0062 Å Wavelength=0.71073

Cell: a=7.987(2) b=9.9530(12) c=12.6520(6)  
alpha=81.935(4) beta=89.228(6) gamma=79.397(15)

Temperature: 100 K

	Calculated	Reported
Volume	978.7(3)	978.7(3)
Space group	P -1	P -1
Hall group	-P 1	-P 1
Moiety formula	C24 H19 Cl Fe N2 O2	C20 H20 Fe1 O4 Se1
Sum formula	C24 H19 Cl Fe N2 O2	C24 H19 Cl Fe N2 O2
Mr	458.71	458.71
Dx,g cm-3	1.557	1.557
Z	2	2
Mu (mm-1)	0.925	0.932
F000	472.0	472.0
F000'	473.13	
h,k,lmax	10,12,16	10,12,16
Nref	4342	4342
Tmin,Tmax		
Tmin'		

Correction method= Not given

Data completeness= 1.000 Theta(max)= 27.150

R(reflections)= 0.0520( 3066) wR2(reflections)= 0.1379( 4020)

S = 1.058 Npar= 348

The following ALERTS were generated. Each ALERT has the format

**test-name\_ALERT\_alert-type\_alert-level.**

Click on the hyperlinks for more details of the test.

** Alert level A**

PLAT029\_ALERT\_3\_A \_diffrn\_measured\_fraction\_theta\_full Low ..... 0.926

**Author Response: Data were collected on a synchrotron**

---

**Alert level C**

PLAT222_ALERT_3_C	Large Non-Solvent	H	Uiso(max)/Uiso(min) ..	4.6	Ratio
PLAT245_ALERT_2_C	U(iso) H5	Smaller than U(eq)	C5 by ...	0.012	AngSq
PLAT245_ALERT_2_C	U(iso) H10	Smaller than U(eq)	C10 by ...	0.020	AngSq
PLAT245_ALERT_2_C	U(iso) H21	Smaller than U(eq)	C21 by ...	0.027	AngSq
PLAT341_ALERT_3_C	Low Bond Precision on	C-C Bonds .....		0.0062	Ang

---

**Alert level G**

FORMU01\_ALERT\_1\_G There is a discrepancy between the atom counts in the  
 \_chemical\_formula\_sum and \_chemical\_formula\_moiety. This is  
 usually due to the moiety formula being in the wrong format.  
 Atom count from \_chemical\_formula\_sum: C24 H19 Cl1 Fe1 N2 O2  
 Atom count from \_chemical\_formula\_moiety:C20 H20 Fe1 O4 S1

ABSMU\_01 Radiation type not identified. Calculation of  
 \_exptl\_absorpt\_correction\_mu not performed.

PLAT002_ALERT_2_G	Number of Distance or Angle Restraints on AtSite	4
PLAT005_ALERT_5_G	No _iucr_refine_instructions_details in CIF ...	?
PLAT042_ALERT_1_G	Calc. and Reported MoietyFormula Strings Differ	?
PLAT164_ALERT_4_G	Nr. of Refined C-H H-Atoms in Heavy-Atom Struct.	17
PLAT232_ALERT_2_G	Hirshfeld Test Diff (M-X) Fe1 -- C17	6.5 su
PLAT860_ALERT_3_G	Note: Number of Least-Squares Restraints .....	2
PLAT984_ALERT_1_G	The Fe-f' = 0.346 Deviates from the B&C-Value	0.348

---

1 **ALERT level A** = Most likely a serious problem - resolve or explain  
 0 **ALERT level B** = A potentially serious problem, consider carefully  
 5 **ALERT level C** = Check. Ensure it is not caused by an omission or oversight  
 8 **ALERT level G** = General information/check it is not something unexpected

3 ALERT type 1 CIF construction/syntax error, inconsistent or missing data  
 5 ALERT type 2 Indicator that the structure model may be wrong or deficient  
 4 ALERT type 3 Indicator that the structure quality may be low  
 1 ALERT type 4 Improvement, methodology, query or suggestion  
 1 ALERT type 5 Informative message, check

---

## checkCIF publication errors

---

**Alert level A**

PUBL004\_ALERT\_1\_A The contact author's name and address are missing,  
 \_publ\_contact\_author\_name and \_publ\_contact\_author\_address.

PUBL005\_ALERT\_1\_A \_publ\_contact\_author\_email, \_publ\_contact\_author\_fax and  
 \_publ\_contact\_author\_phone are all missing.  
 At least one of these should be present.

PUBL006\_ALERT\_1\_A \_publ\_requested\_journal is missing  
 e.g. 'Acta Crystallographica Section C'

PUBL008\_ALERT\_1\_A \_publ\_section\_title is missing. Title of paper.

PUBL009\_ALERT\_1\_A \_publ\_author\_name is missing. List of author(s) name(s).

PUBL010\_ALERT\_1\_A \_publ\_author\_address is missing. Author(s) address(es).

PUBL012\_ALERT\_1\_A \_publ\_section\_abstract is missing.  
 Abstract of paper in English.

---

**Alert level G**

PUBL013\_ALERT\_1\_G The \_publ\_section\_comment (discussion of study) is

missing. This is required for a full paper submission (but is optional for an electronic paper).

PUBL017\_ALERT\_1\_G The `_publ_section_references` section is missing or empty.

- 7 **ALERT level A** = Data missing that is essential or data in wrong format  
 2 **ALERT level G** = General alerts. Data that may be required is missing

## Publication of your CIF

You should attempt to resolve as many as possible of the alerts in all categories. Often the minor alerts point to easily fixed oversights, errors and omissions in your CIF or refinement strategy, so attention to these fine details can be worthwhile. In order to resolve some of the more serious problems it may be necessary to carry out additional measurements or structure refinements. However, the nature of your study may justify the reported deviations from journal submission requirements and the more serious of these should be commented upon in the discussion or experimental section of a paper or in the "special\_details" fields of the CIF. *checkCIF* was carefully designed to identify outliers and unusual parameters, but every test has its limitations and alerts that are not important in a particular case may appear. Conversely, the absence of alerts does not guarantee there are no aspects of the results needing attention. It is up to the individual to critically assess their own results and, if necessary, seek expert advice.

If level A alerts remain, which you believe to be justified deviations, and you intend to submit this CIF for publication in Acta Crystallographica Section C or Section E, you should additionally insert an explanation in your CIF using the Validation Reply Form (VRF) below. Your explanation will be considered as part of the review process.

If you intend to submit to another section of Acta Crystallographica or Journal of Applied Crystallography or Journal of Synchrotron Radiation, you should make sure that at least a basic structural check is run on the final version of your CIF prior to submission.

```
# start Validation Reply Form
_vrf_PUBL004_GLOBAL
;
PROBLEM: The contact author's name and address are missing,
RESPONSE: ...
;
_vrf_PUBL005_GLOBAL
;
PROBLEM: _publ_contact_author_email, _publ_contact_author_fax and
RESPONSE: ...
;
_vrf_PUBL006_GLOBAL
;
PROBLEM: _publ_requested_journal is missing
RESPONSE: ...
;
_vrf_PUBL008_GLOBAL
;
PROBLEM: _publ_section_title is missing. Title of paper.
RESPONSE: ...
;
_vrf_PUBL009_GLOBAL
;
```

```

PROBLEM: _publ_author_name is missing. List of author(s) name(s).
RESPONSE: ...
;
_vrf_PUBL010_GLOBAL
;
PROBLEM: _publ_author_address is missing. Author(s) address(es).
RESPONSE: ...
;
_vrf_PUBL012_GLOBAL
;
PROBLEM: _publ_section_abstract is missing.
RESPONSE: ...
;
# end Validation Reply Form

```

If you wish to submit your CIF for publication in Acta Crystallographica Section C or E, you should upload your CIF via the web. If your CIF is to form part of a submission to another IUCr journal, you will be asked, either during electronic submission or by the Co-editor handling your paper, to upload your CIF via our web site.

---

**PLATON version of 22/10/2012; check.def file version of 16/10/2012**

Datablock I - ellipsoid plot

